Indian Journal of Science and Technology http://www.indjst.org Vol.1 No.2 (Dec. 2007)

The synthesis and characterization of titanium dioxide nanoparticles as potential photosensitizer in photodynamic therapy

[#]Karunakaran Sulochana Meena, [$]Prakasa Rao Aruna, [*]Velayutham Murugesan, [*]Thyagarajan Venkataraman, [$] Singaravel Ganesan.
[#]*Department of Chemistry, Queen Mary's College, Chennai,*
[$]*Department of Physics-;* [*] *Department of Chemistry- Anna University, Chennai,*
[*]*Department of Chemistry, Adhiparasakthi College of Science, Kalavai*
Email: meengiri@yahoo.com

Abstract: TiO_2 nano-photosensitizer particles less than 10nm have been synthesized and characterized. They were prepared by hydrolysing Titanium (IV) isopropoxide in presence of ultrasonic waves and further characterized by absorption and fluorescence spectroscopy, XRD, FTIR, TGA, DSC, SEM, and HRTEM techniques. The XRD patterns revealed exclusive formation of anatase without contamination by rutile form. High resolution transmission electron microscopic measurements revealed their size below 10nm. The photohemolysis induced by TiO_2 NPs reveals that the percent hemolysis increased with the increase in concentration and light dose. The study of effect of scavengers, GSH and NaN_3 showed the formation of considerable amount of superoxide anion and singlet oxygen that caused cell death. The mechanism has been discussed. TiO_2 nano-photosensitizer being non-toxic, serves as proper substitute for the classical photosensitizers (organic dyes).

Introduction

Photodynamic therapy (PDT) is one of the emerging treatment modalities for cancer that takes advantage of the interaction between light and a photosensitizing agent to initiate cell death (Morris *et al*., 2003; Dougherty *et al*., 1998). The conventional photosensitizers viz., diheaemato porphyrin ester, protoporphyrin-IX, ALA induced endogenous proto porphyrin IX and the other second generation photosensitizers such as phthalocyanines and nanpahthalocyanines (Pushpan *et al*., 2002; Ackroyd *et al*., 2001) have their own limitations. They showed poor absorption cross section in the red region and poor triplet quantum yield. Most of them tend to aggregate in aqueous solutions thus leading to loss of photochemical activity and reduction in cell penetrating properties (Allen *et al*., 2001; Roy *et a*l., 2003). Most of the classical photosenisitizers are generally not chemically pure and undergo photobleaching (Konig *et al*., 1990) during light irradiation. Their photodynamic activity is thus affected considerably. Furthermore, the remaining sensitizers after PDT can migrate to skin and eyes and make the patient very sensitive to day light. This effect can last even for one or two months. In this context, to overcome such drawbacks of conventional photosensitizers, many researchers in recent years have considered the possibility of using the non-toxic semi conducting nanoparticles in PDT (DeRosa & Crutchley, 2002; Kawahara *et al*., 2003; Zeitouni, 2003) and it is often referred as nano-PDT. It is a promising route to overcome many difficulties associated with traditional PDT. This is because the nanoparticles are having the following advantages over the conventional photosensitizers. Generally they are photostable and nontoxic even though recent investigation attributes its differential biological behaviour with variable molecular size (Gurr *et al*., 2005). They also have large absorption cross section, good photoluminescence quantum yields and long emission lifetimes. Due to their adjustable surface chemistry, they can be modified to become water soluble biocompatible (Wang *et al*., 2004) and target specific. However, the use of nanoparticles in nano-PDT is still under primitive stage. This paper reports the synthesis and characterization of TiO_2-NPs; their photodynamic activity on human erythrocytes was also studied as the function of light and drug doses. Further, attempt was made to understand the mechanism involved in nano-PDT using TiO_2-NPs as photosensitizer.

Materials and Methods

Preparation of TiO_2 – nanoparticles

Titanium (iv) isopropoxide was purchased from Sigma Aldrich and all the other reagents used in this experiment were Analar grade. Double deionised water was used. TiO_2 nanoparticles were prepared by slight modification of the method described by Weijun Liu *et al* (1999). In brief, titanium(iv) isopropoxide (5ml) was dissolved in ethanol (5ml) and then hydrolysed at room temperature by adding it to hydrochloric acid (30ml, 0.1M) solution drop wise under stirring. The slurry obtained was refluxed at 70°C for 6 hours with constant vortex. The colloidal solution obtained was sonicated for about 5 hours and filtered on a glass frit to remove non-peptized agglomerate. The filtrate

obtained was evaporated to get a gel which was then calcined to get a white powder of TiO_2-NPs. The TiO_2 nanoparticles synthesized were characterized by UV-Visible absorption and emission spectroscopy, FTIR, TGA, XRD, SEM, and HRTEM.

Fig.1. UV-Visible Absorption Spectrum of TiO_2-NPs

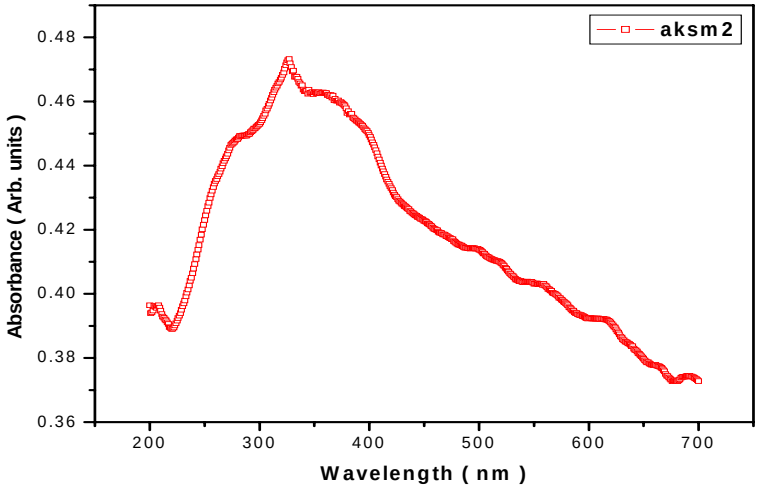

UV-visible spectra were recorded in a spectrophotometer (Perkin Elmer Lambda 35). The fluorescence spectra were recorded using spectrofluorimeter (FluoroMax-2, SPEX, USA). X-ray diffraction (XRD) patterns were taken from X'pert PRO PANalytical diffractometer operating with CuKα radiation (λ=1.5406A°) source. FTIR spectroscopic measurements were carried out with a Perkin Elmer FTIR Spectrum RXI spectrometer. Thermogravimetric analysis (TGA) was performed using WATERS SDT Q600 thermal analysis instrument. About 10-20 mg of sample was used at a heating rate of 10° C /min and the data were collected between 35 and 1000°C. The measurements were made in N_2 atmosphere.

DSC measurements were carried out in a WATERS DSC Q10 Differential Scanning Calorimeter in oxygen. High resolution transmission electron microscopy (HRTEM) photographs were taken using a JEOL JEM - 3010 Electron microscope operating at 300 keV. The magnifying power used was 600 and 800k times.

Preparation of PBS

Phosphate buffered saline (PBS) was prepared by mixing 280ml of 0.2M monobasic sodium phosphate, 720ml of 0.2M dibasic sodium phosphate along with 9g of sodium chloride and the pH was found to be 7.3. All the solutions were prepared in PBS.

Erythrocyte separation

Fresh human blood was obtained from healthy volunteers from Health Centre of Anna University in Chennai, and mixed with anticoagulant EDTA in the ratio 3:1. The erythrocytes were allowed to settle for an hour and the plasma leukocytes and thrombocytes were separated by aspirating the supernatant. The sediment was washed 4-5 times with PBS to remove any left out plasma. A stock solution of 0.5% erythrocyte suspension was prepared by diluting 2ml of the solution with 38ml of PBS.

Sample irradiation

Light from Xenon source filtered at 445 nm with 20 nm bandpass filter was used for irradiating the samples. The microtitre plates having wells of 2.5cm diameter containing 1ml of the sample were irradiated at different light dose and concentrations of TiO_2 nanoparticles. The irradiated cell suspension was centrifuged at 1500 rpm for 10min and the supernatant was pipetted out and its O.D at 413nm was measured using a spectro photometer to quantify the percent hemolysis. The same procedure was repeated to study the role of scavengers such as sodium azide (Wilkinson & Brummer, 1981) and Glutathione reduced (GSH) (Islam *et al.*, 1997) by adding 1ml of each scavenger separately with 1ml of TiO_2 nanoparticles in PBS during hemolysis.

Results and discussion

Characterization of TiO_2-nanoparticles

UV-Visible absorption spectrum of TiO_2-NPs: The UV-Visible absorption spectrum of TiO_2-NPs was scanned between 200 and 700nm (Fig.1). The absorption maximum occurs at 340nm which shows a band gap value of 3.6 eV.

DRS UV-Visible spectrum:The DRS-UV-Visible spectral analysis of TiO_2-NPs was carried out between 200 and 700nm.The plot of absorbance verses wave length is shown in Fig.2. The spectrum illustrates increase in absorbance just below 400nm due to band gap excitation. By taking 350nm as the onset of absorbance the band gap value was calculated to be 3.5eV. The band gap value is consistent with that of UV-Visible absorption spectrum of TiO_2- NPs (Fig.1). Sharp absorbance lines below 250nm are due to TiO_2 particles of size much smaller than those absorbing close to 350nm.

Fig.2. DRS-UV-Visible absorption spectrum of TiO_2-NPs

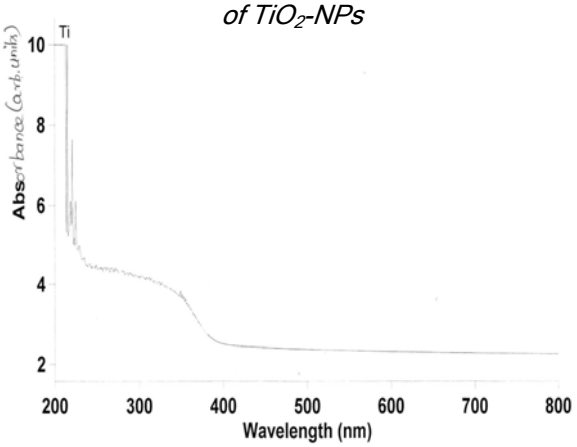

Fig.3(a). Fluorescence spectrum of TiO_2-NPs excited at 300nm

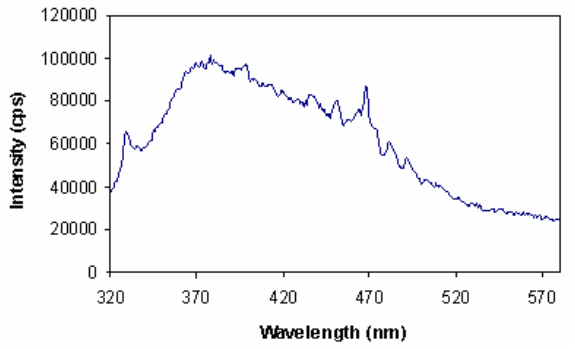

Steadystate Fluoresence Spectroscopic characteristics of TiO_2 - Nanoparticles: The fluorescence spectrum of TiO_2-NPs, excited at 300nm, is shown in Fig.3(a). The fluorescence gives a broad maximum close to 380nm. It is also close to band gap excitation shown in Fig.2. Hence TiO_2-NPs after excitation gives maximum fluorescence only from the levels close to the lowest level of the conduction band. Again there is significant fluorescence at about 470 nm. The fluorescence spectrum of TiO_2-NPs excited at 330nm is shown in Fig.3(b). It depicts nearly similar features as that of Fig 3(a). The florescence maximum lies close to 370nm.

Fig.3(b). Fluorescence spectrum of TiO_2-NPs excited at 330nm

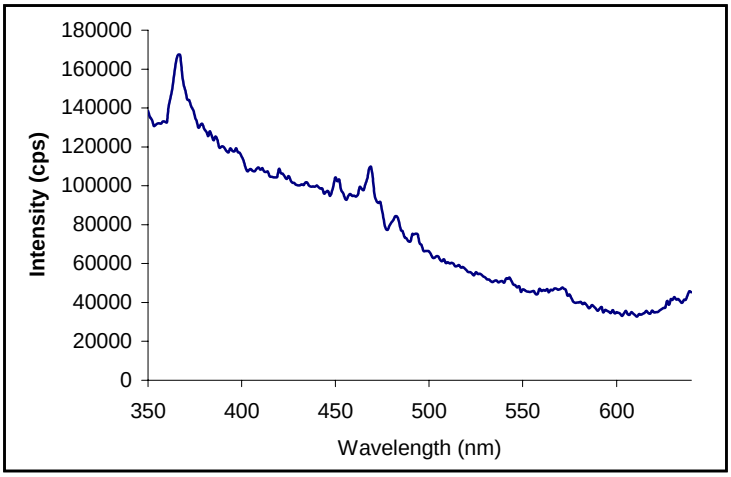

XRD analysis of TiO_2-NPs: The XRD pattern of TiO_2-NPs calcined 120ºC is shown in Fig.4. The patterns are very well comparable to anatse form of TiO_2-NPs reported in the literature (Weijun *et al*., 1999). The phase is completely free of rutile form. The signals appear to be rather broad due to the nano size. The five characteristic peaks at (2θ) about 25.63, 38.23, 48.08, 54.4 and 62.9° correspond to anatase the form of TiO_2 (JCPDS # 89-4921), tetragonal structure with body centered cubic lattice with cell parameters a = 3.777 & c = 9.501. The space group was found to be 141/omd (141). The average crystal grain size calculated using the Scherrer equation was found to be 6.02nm which is well in accordance with HRTEM photographs of TiO_2-NPs in Fig. 8.

FTIR Spectroscopy: The TiO_2-NPs were characterized by taking FTIR spectrum of the calcined (120ºC) sample. The spectrum was recorded in KBr matrix. The FTIR spectrum of TiO_2-NPs is shown in Fig 5. The bands centered at 3284 $cm^{-1}$and 1618 cm^{-1} are characteristic of u-OH stretching and δ-H_2O bending respectively. The Ti-O vibration appears as a broad envelope between 1000-400cm^{-1}. Since there is no C-H vibration band from 3000 to 2700 cm^{-1}, the TiO_2-NPs are free of adsorbed organics. We can thus consider that the hydrolysis reaction leads to Ti $(OH)_4$ n.H_2O precursor. The spectrum is very well comparable with that given by Guillaume Sudant *et al*. (2005).

Thermo Gravimetry Analysis (TGA): The TGA of the air dried TiO_2 NPs has been carried out between 50 and 900°C. The TGA trace of TiO_2-NPs is shown in Fig.6. There is a weight loss between 50-150°C due to desorption of adsorbed water. There is a gradual increase in weight loss from 300 to about 550°C. It is assigned to condensation of adjacent defective-OH groupings on the crystal surface. It also supports FTIR results described above. Again there is another weight loss from 600-750°C. It is ascribed to condensation of defective-OH groupings which may not be very close. Thus the thermogravimetric

study of TiO_2 - NPs shows a monotonous mass decrease with temperature and is well comparable with that reported in the literature (Sudant *et al.*, 2005).

Fig.4. X-Ray diffraction patterns of TiO_2 -NPs dried at 120ºC

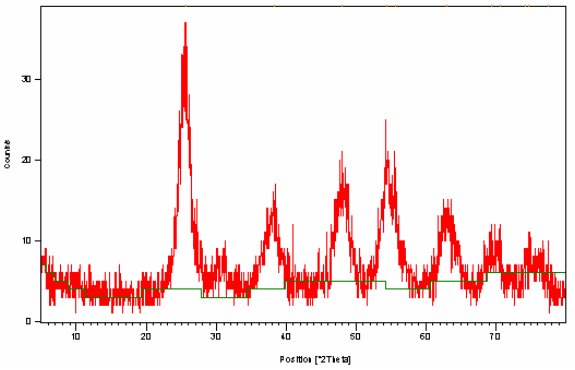

Fig.5. FTIR spectrum of air dried TiO_2 -NPs

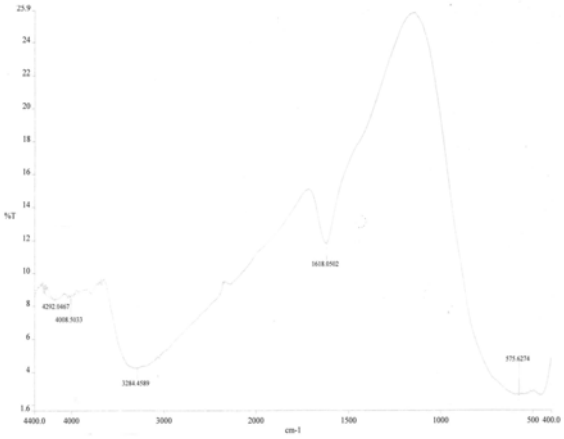

Differential Scanning Colorimetry (DSC): The DSC analysis was carried out in the temperature range 50 and 400°C. There is an endothermic peak between 50 and 125°C (Fig.7). This endothermic peak coincides with the first major weight loss in the TGA trace shown in Fig.6. It is due to loss of adsorbed water. There is also a broad endotherm above 250°C. It is assigned to condensation of the adjacent defective Ti-OH groupings on the surface. It also supports the results of TGA as discussed above.

HR-TEM Pictures of TiO_2-NPs: The microstructure of TiO_2-NPs is illustrated by the HRTEM images. The HRTEM images of TiO_2-NPs are shown in Fig 8(a). All the images clearly illustrate particles of nearly uniform size. The particles are aggregated but the boundary between them is clearly seen. Fig.8(b) shows the lattice planes of anatase crystallite of TiO_2-NPs. The particle size varies from 4-5nm.This size is also comparable to that derived by Sherrer equation in the XRD analysis.

Photohemolysis using TiO_2-NPs

The rate of photohemolysis was carried out in vitro under two different experimental conditions i) at different light dose (23,46,68 Jcm^{-2}) at fixed concentrations of TiO_2 - NPs, and ii) at different TiO_2 concentrations (50, 100 and 150 µg/ml) at fixed light dose.

Photohemolysis as the function of light dose: At

Fig.6. TGA thermogram of air dried TiO_2 -NPs

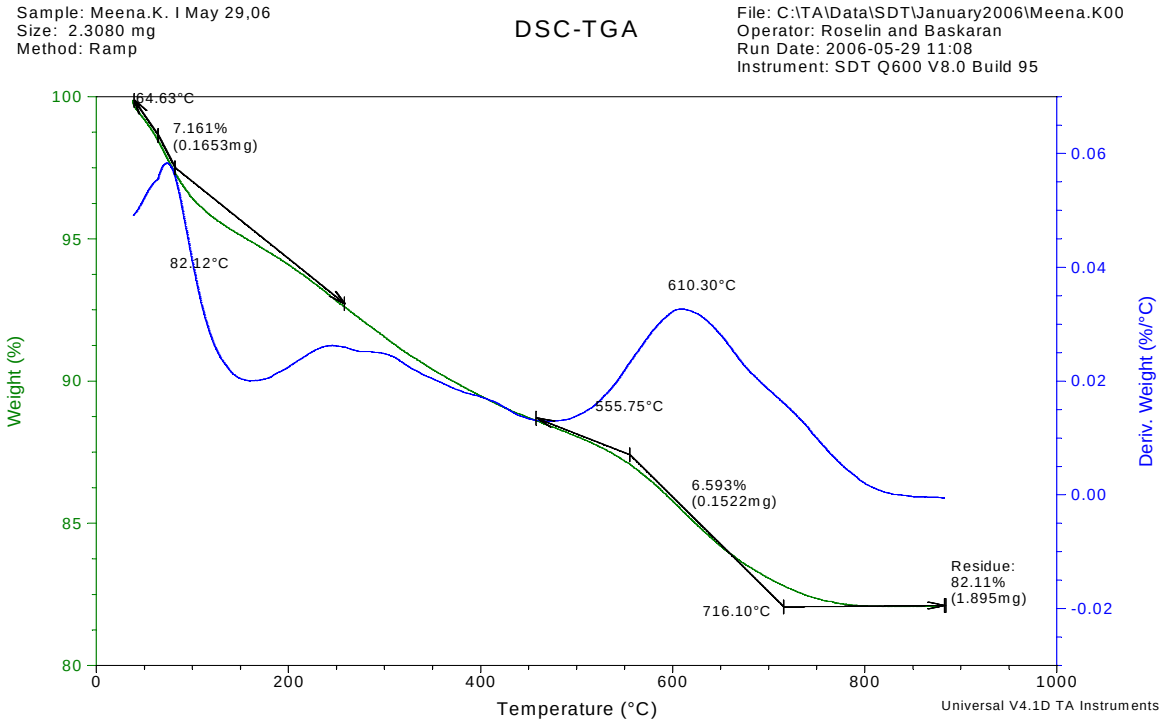

50 µg/ml TiO_2-NPs the percent hemolysis remains almost the same, i.e., around 12-15% (Fig 9) at all light doses. On increasing the concentration from 50µg/ml to 100µg/ml and for 23Jcm^{-2} light dose the percent hemolysis slightly increased. At higher light doses (46, 68Jcm^{-2}) and for the same concentration of NPs there was a considerable increase in the percent hemolysis (Fig 9). Hence it is observed that

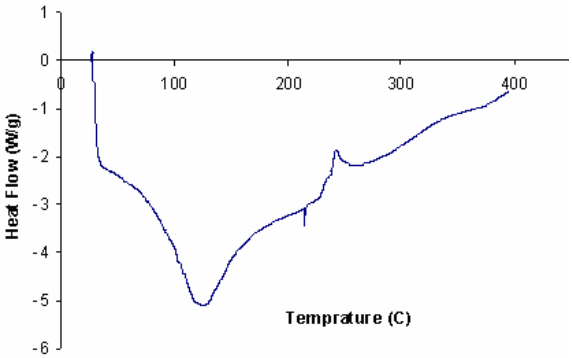

Fig.7. DSC Thermogram of air dried TiO_2 - NPs

optimization of both the concentration of TiO_2-NPs and the light dose is important to increase the photohemolysis considerably. From figure 9, the LD_{50} (Lethal for 50% hemolysis) is found to be 48 Jcm^{-2} and 57 Jcm^{-2} for 150 µg/ml and 100 µg/ml concentration of TiO_2-NPs respectively.

8(a,b).High resolution transmission electronic microscopy picture of TiO_2-NPs

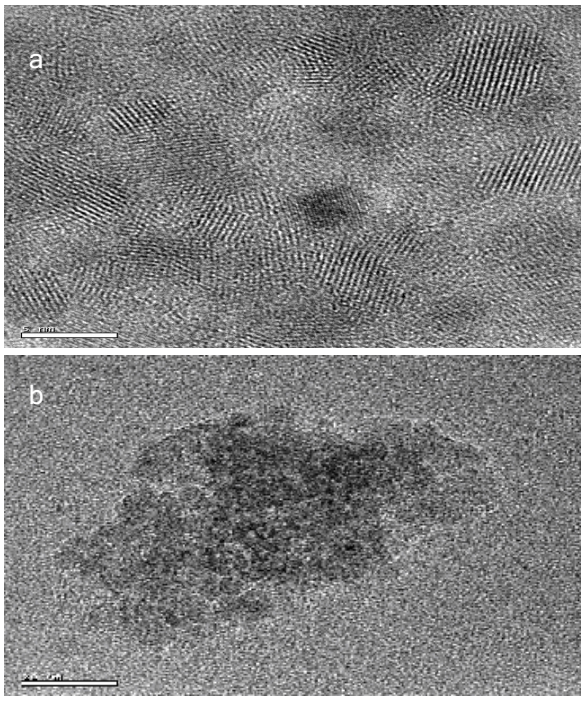

This shows that light dose is considerably reduced when the sensitizer concentration is increased from 100µg/ml to 150µg/ml. The size of TiO_2-NPs (below 10nm), the concentration limits and the exposure time which were used in the study are much lesser than that reported by Ai-Ping Zhang *et al*., (2005). Further visible light is used instead of UV as the latter may induce harmful effect.

Photohemolysis as the function of concentration of nano-sensitizer: Fig.10 shows the variation of photohemolysis with concentration of TiO_2-NPs at fixed light doses. It is clearly observed that photolysis increases with concentration as well as with fluence. The LC_{50} (lethal concentration of NP for 50% hemolysis) is achieved only at 46 Jcm^{-2} and at 68 Jcm^{-2}. The LC_{50} values are 150µg/ml and 78µg/ml for light doses 46 Jcm^{-2} and 68 Jcm^{-2} respectively. This clearly indicates that at 68 Jcm^{-2} the concentration required to produce 50% hemolysis is reduced to almost half of the concentration that needed for 46 Jcm^{-2}. From Fig. 9 & 10 it is clearly observed that TiO_2-NP induces lysis effectively even at lesser doses than that required by conventional photosensitizers. As the lysis depends both on light dose as well as on concentration of the nano photosensitizer, the nature of photohemolysis is purely a chemical medicated one either by Type I or / and Type II mechanisms.

Effect of scavengers

In order to know whether TiO_2-NPs favours Type-I and/or Type-II mechanism, the photohemolysis was carried out in the presence of scavengers, GSH and NaN_3 which are the best known quenchers for superoxide anion and singlet oxygen ($^1O_2$) respectively. The inhibition of photohemolysis was calculated by taking the corresponding percentage hemolysis without scavenger as 100%. Fig 11. shows the role of scavenger NaN_3, at various concentrations of TiO_2-NPs. When the photohemolysis of 50 µg/ml of TiO_2-NPs for 46 Jcm^{-2} light dose was carried out along with 1 ml of 45mM NaN_3, the photohemolysis was reduced to 70%. When the concentration of NaN_3 was increased to 90mM for the 50 µg/ml TiO_2, the percent hemolysis further reduced to 52.5%. The inhibition of photohemolysis with 100 µg/ml and 150 µg/ml TiO_2-NPs along with 45 and 90mM NaN_3 was also carried out. The percent hemolysis was reduced to 30-35% in almost all the cases. This clearly shows that photohemolysis using TiO_2 - NPs involves the formation of singlet oxygen which is quenched by sodium azide scavenger.

The mechanism of singlet oxygen induced toxicity has also been documented earlier (Konaka *et al*., 2001).

Fig.9. Effect of light dose on photohemolysis of TiO_2-NPs

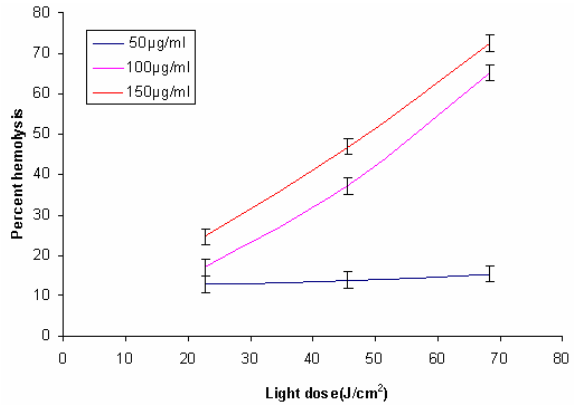

Fig.10. Effect of concentration on photohemolysis of TiO_2-NPs

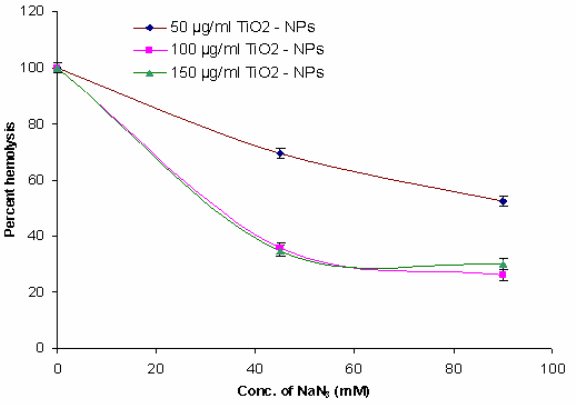

When the photohemolysis with TiO_2-NPs was carried out with 20mM GSH, for all the concentrations of TiO_2 the percent of hemolysis reduced to 30 – 35% (Fig.12). The concentration of GSH was increased from 20 to 40mM for various TiO_2-NPs concentration. The percent hemolysis with 50 and 100 µg/ml TiO_2-NPs was reduced nearly to 15% and with 150µg/ml

Fig.11. Effect of scavenger NaN_3 on photohemolysis of TiO_2-NPs

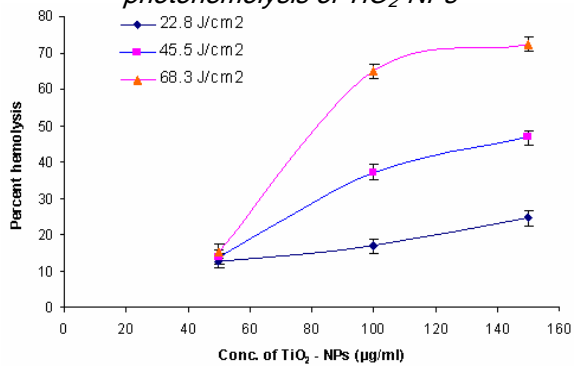

reduced to 7% for 40mM GSH concentration. This clearly indicates the formation of the superoxide anion in all the cases.

A control experiment was carried out with different concentrations of TiO_2 -NPs without irradiation and it is confirmed that non-irradiated TiO_2 -NPs are not toxic to

Fig.12. Effect of scavenger GSH on photohemolysis of TiO_2-NPs

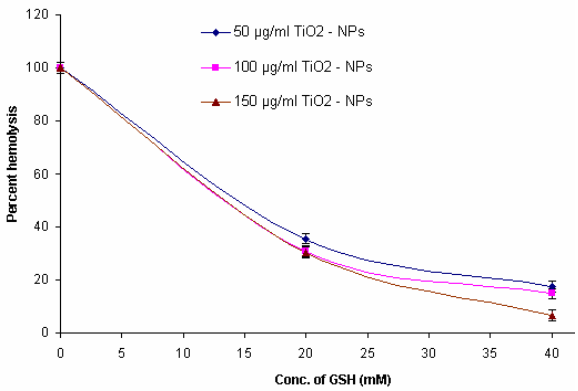

erythrocytes. Similarly the non-irradiated TiO_2 -NPs with scavengers also show no cell killing effect.

It was observed that in both cases, as the concentration of scavengers increased the percent hemolysis decreased to a considerable amount. Comparing the effects of scavengers GSH & NaN_3 in the inhibition of photohemolysis, the inhibition effect is more with the former than the latter. Therefore it is confirmed that even though both superoxide anion and $^1O_2$ are formed during hemolysis which are the major cause for hemolysis of erythrocytes, superoxide anion radical is formed more since GSH showed more inhibition effect than NaN_3. Therefore the photohemolysis of human erythrocytes using TiO_2 -NPs follows both type I and type II mechanisms and the former one more predominating than the latter.

Conclusion

Nanosize TiO_2 particles (below 10nm) were prepared, characterized and used as a nano-photosensitizer in the place of organic dyes in Photodynamic therapy. In the present study human erythrocyte cells were effectively hemolysed by photoexcited TiO_2-NPs. The photolysing of erythrocytes was considerably affected by the concentration of TiO_2-NPs and light dose. When the concentration is increased from 50 to 100 and then to 150µg/ml for 23 to 68Jcm^{-2} light dose the maximum percentage hemolysis achieved was nearly 73%. The role of scavengers such as GSH and NaN_3 indicates that there is a considerable formation of superoxide anion and singlet oxygen during

photoexitation of TiO_2-NPs. While comparing the effects of scavengers, the inhibition of the photohemolysis is higher with GSH. Hence it is concluded that photo-induced cell killing of red blood cells by TiO_2-NPs favours both Type I & Type II mechanisms and the former one predominates than the latter. The unexposed TiO_2-NPs were found to be nontoxic towards red blood cells. The study concludes that light irradiated TiO_2-NPs can be a convenient substitute for the conventional photosensitizers such as organic dyes.

References

1. Ackroyd R, Kelty C, Brown N, and Reed M. (2001) The History of Photodetection and Photodynamic Therapy, *Photochemistry and Photobiology* 74, 656-669.
2. Ai-Ping Zhang and Yan-Ping Sun (2004) Photokilling effect of TiO_2 nanoparticles on Ls-174-t human colon carcinoma cells. *World. J. Gastroenterol.*, 10, 3191-3193.
3. Allen, CM, Sharman WM and Van Lier JE (2001) *J. Porphyrins Phthalocyanines* 5, 161.
4. DeRosa MC and Crutchley RJ (2002) *Coord. Chem. Rev.,* , 233-234,351.
5. Dougherty TJ, Gomer CJ, Henderson BW, Jori G, Kessel D, Korbelik M, Mean J and Peng Q. (1998) *J. Natl*, *Cancer Inst.*90, 889.
6. Guillame Sudant, Emmanuel Baudrin, Dominique Larcher and Jean-Marie Tarascon (2005) Electrochemical Lithium reactivity with nanotextured anatase-type TiO_2, *J. Mater. Chem.*15,1263-1269.
7. Gurr J-R, Wang ASS, Chenb C-H, Jan K-Y (2005) Ultrafine titanium dioxide particles in the absence of photoactivation can induce oxidative damage to human bronchial epithelial cells. *Toxicology* 213, 66–73.
8. Islam KN, Kayanoki Y, Kaneto H, Suzuki K, Asahi M, Fijii J and Taniguchi N (1997) TGF-betal triggers oxidative modifications and enhances apoptosis in HIT cells through accumulation of reactive oxygen species by suppression of Catalase and glutathione peroxidase, *Free Radic Biol.Med.* 22,1007-1017.
9. Kawahara T, Ozawa T, Iwasaki M, Tada H, Ito S (2003) Photocatalytic activity of rutile–anatase coupled TiO2 particles prepared by a dissolution-reprecipitation method. *J. Colloid Interf. Sci.* 267, 377–381.
10. Konaka R, Kasahara E, Dunlap WC, YamamotoY, Chien KC and Inoue M (2001) Ultraviolet irradiation of titanium dioxide in aqueous dispersion generates singlet oxygen. *Redox Rep*. 6, 319-325.
11. Konig K, Wabnitz H and Dietel W (1990) *J.Photochem.Photobiol, B*. 8,103.
12. Morris RL, Azizuddin K, Lam M, Berlin J, Nieminen A, Kenny ME, Samia ACS, Burda C, Oleinick NL. (2003) Fluorescence resonance energy transfer reveals a binding site of a photosensitizer for photodynamic therapy. *Cancer Res.* 63, 5194-5197.
13. Pushpan SK, Venkatraman S, Anand VG, Sankar J, Parmeswaran D, Genesan S and Chandrashekar TK (2002) Porphyrins in Photodynamic Therapy – A search for Ideal Photosensitizers. *Curr. Med. Chem. – Anti-Cancer Agents.* 2, 187-207.
14. Roy I, Ohulchanskyy TY, Pudavar HE, Bergy EJ, Oseroff AR, Morgan J, Dougherty TJ, Prasad PN (2003) *J.Am.Chem.Soc.* 125,7860.
15. Wang S, Gao R, Zhou F, and Selke M (2004) Nanomaterials and singlet oxygen photosensitizers, potential application in PDT. *J. Mater. Chem.* 14, 487-493.
16. Weijun Liu, Yuan Wang, Linlin Gui and Youqi Tang (1999) Preparation and Characterisation of Novel Nanoscopic Titanium Dioxide / Phthalocyanine Complex Films, *Langmuir* 15, 2130-2133.
17. Wilkinson F, and Brummer JG (1981) Rate constants for the decay and reactions of the lowest electrically excited singlet state of molecular oxygen in solution. *J. Phys. Chem.* 10, 809-999.
18. Zeitouni NC, Oseroff AR and Shieh S. (2003) Photodynamic therapy for nonmelanoma skin cancers. Current review and update. *Mol. Immunol.* 39,1133-1136.